Available online at www.sciencedirect.com
SCIENCE DIRECT
Inorganica Chimica Acta 359 (2006) 3800–3806
Inorganica Chimica Acta
www.elsevier.com/locate/ica

A kinetic investigation of the oxidative addition reactions of the dimeric $Bu_4N[Ir_2(\mu\text{-Dcbp})(cod)_2]$ complex with iodomethane

Ebeth Grobbelaar, Walter Purcell *, Stephen S. Basson *

Department of Chemistry, University of the Free State, Bloemfontein 9300, South Africa

Received 3 June 2005; accepted 31 March 2006
Available online 13 May 2006

Abstract

The kinetic results of the oxidative addition of iodomethane to $Bu_4N[Ir_2(\mu\text{-Dcbp})(cod)_2]$ (Dcbp = 3,5-dicarboxylatepyrazolate anion) show that oxidative addition can occur via a direct equilibrium pathway (K_1 = 88(22) acetone, 51(3) 1,2-dichloroethane, 55(4) dichloromethane, 52(12) acetonitrile and 43(5) M^{-1} chloroform) or a solvent-assisted pathway (k_2, k_3). Oxidative addition occurs mainly along the direct pathway, which is a factor 10–40 faster than the solvent-assisted pathway. The observed solvent effect cannot be attributed to the donosity or polarity of the solvents. The fairly negative $\Delta S^{\neq}$ value ($-110(7)$ J K^{-1} mol^{-1}) and the positive $\Delta H^{\neq}$ value ($+47(2)$ kJ mol^{-1}) for the oxidative addition step are indicative of an associative process.

Keywords: Oxidative addition; Iridium; 3,5-Dicarboxylatepyrazolate; Iodomethane; Kinetics

1. Introduction

The possible applications of dimeric complexes such as pyrazolyl-bridged iridium(I) dimers in catalysis have increased tremendously during recent years [1]. In certain cases such as in the hydrogenation of cyclohexene the catalytic activity of the dimeric complexes are higher than that of the corresponding monomeric complexes [2–5]. The higher catalytic activity of the dimeric complexes is attributed to the electronic communication between the metal ions through bridging ligands such as pyrazoles [6].

The presence of two metal ions which can undergo oxidative addition give rise to different oxidative addition patterns such as reversible and irreversible oxidative addition and addition on only one or both metal ions [8]. Co-operative effects between the metal ions could also lead to metal–metal bond formation and/or the migration of the added fragments between the two metal ions [9–12]. In some cases oxidative addition on one metal ion leads to the deactivation of the second metal ion for oxidative addition. This type of deactivation is the result of electron donation from the metal ion in the lower oxidation state to the metal ion in the higher oxidation state. The result of this deactivation is that while one metal ion is activated for oxidative addition the other is activated for reductive elimination, a feature which can be very useful in the design of catalysts [13].

Despite this very attractive feature of the oxidative addition reactions of dimeric pyrazolyl-bridged iridium(I) dimers little is known about the kinetics of these complexes. A kinetic investigation of the oxidative addition reactions of CH_3I to $Bu_4N[Ir_2(\mu\text{-Dcbp})(cod)_2]$ was thus undertaken to gain knowledge about the mechanism and factors which influence the oxidative addition reactions of dimeric complexes. These results were also compared to the oxidative addition reactions of the corresponding monomeric iridium(I) β-diketone complexes done in our laboratory [14].

2. Experimental

2.1. General considerations

All the preparations were performed under an atmosphere of dry nitrogen and unless otherwise stated all the

* Corresponding authors. Fax: +27 51 4307805 (W. Purcell).
E-mail address: purcellw.sci@mail.uovs.ac.za (W. Purcell).

0020-1693/$ - see front matter © 2006 Elsevier B.V. All rights reserved.
doi:10.1016/j.ica.2006.03.041

chemicals were reagent grade and used without further purification. IR spectra were recorded with a Hitachi 270-50 spectrophotometer while the NMR spectra were obtained at 293 K on a Bruker 300 MHz spectrometer.

2.2. Syntheses

2.2.1. Preparation of bis-[μ-chloro-η⁴-cycloocta-1, 5-dieneiridium(I)]

[Ir(μ-Cl)(η⁴-cod)]$_2$ was prepared by a modification of the method published by Bezman et al. [15]. Hydrated iridic acid, $H_2[IrCl_6]\cdot xH_2O$, 5 g (Next Chimica) and 3 g of hydroquinone (Merck) were heated under reflux for 1 h with 180 cm^3 of an ethanol/water (2:1) mixture. The ethanol/water mixture was deoxygenated for half an hour prior to usage. The reaction mixture was refluxed for a further 4 h on addition of 5 cm^3 *cis*,*cis*-1,5-cyclooctadiene. Approximately 100 cm^3 of solvent was distilled from the reaction vessel and 10 cm^3 of water was added, causing the crystallisation of an orange solid. After cooling the reaction mixture to room temperature, the solid was filtered and washed thoroughly with cold methanol. The product was dried over P_2O_5 in a vacuum desiccator for ca. 15 h. Yield: 72%, ^{1}H NMR ($CDCl_3$), δ 4.18 ppm CH(m), δ 2.20, 1.60 ppm CH_2(m).

2.2.2. Preparation of tetrabutylammonium μ-3, 5-dicarboxylatopyrazolatobis[η⁴-cycloocta-1, 5-dieneiridate(I)], $Bu_4N[Ir_2(\mu\text{-Dcbp})(cod)_2]$

The preparation of $Bu_4N[Ir_2(\mu\text{-Dcbp})(cod)_2]$ by Bayón et al. [16] was modified as follows: 0.2 mmol pyrazole-3,5-dicarboxylic acid (Aldrich) was dissolved in 6 cm^3 0.1 M Bu_4NOH (Merck) and stirred in a nitrogen atmosphere for ca. 1 min to form the pyrazole-3,5-dicarboxylatepyrazolate anion. [Ir(μ-Cl)(η⁴-cod)]$_2$ (0.2 mmol) was dissolved in 5 cm^3 of acetonitrile and added dropwise (slowly) to the pyrazole-3,5-dicarboxylatepyrazolate solution. The solution was stirred for a further 10 min in a nitrogen atmosphere and the bright yellow solid was filtered off. The product was washed with hexane and dried over P_2O_5 in a vacuum desiccator for ca. 15 h. Yield: 60%. ν_{OCO}1642 cm^{-1}, ^{1}H NMR ($CDCl_3$), δ 6.85 ppm H(s), δ 4.10 ppm CH(m) (cod), δ 2.17(m), 1.35–1.70 ppm CH_2(m) (cod), 1.23 ppm (d), δ 1.35–1.70 ppm (m), δ 3.20 CH_2(m) Bu_4N, δ 1.00 ppm CH_3(t) Bu_4N.

2.2.3. Preparation of tetrabutylammonium iodo-η⁴-cycloocta-1,5-dieneiridate(II)-μ-3, 5-dicarboxylatopyrazolatomethyl-η⁴-cycloocta-1, 5-dieneiridate(II), $Bu_4N[(cod)Ir(I)\text{-}\mu\text{-}Dcbp\text{-}Ir(cod)(CH_3)]$

$Bu_4N[Ir_2(\mu\text{-Dcbp})(cod)_2(CH_3)I]$ was prepared as follows: 0.02 mmol $Bu_4N[Ir_2(\mu\text{-Dcbp})(cod)_2]$ was dissolved in 5 cm^3 chloroform (Merck) and a 40-fold excess CH_3I was added to this solution. The solution was heated to 35°C and left for 2 h to allow the oxidative addition to go to completion. The solution was filtered and the solvent removed with nitrogen gas. The yellow/orange oily product was redissolved in 3 cm^3 chloroform, filtered and the solvent removed with nitrogen gas. The product was dried over P_2O_5 in a vacuum desicator for 14 h. Yield: 50%. ^{1}H NMR ($CDCl_3$), δ 6.90 ppm H(s), δ 4.35 ppm CH(m) (cod), δ 2.61(m), 1.30–1.80 ppm CH_2(m) (cod), 1.22 ppm (d), δ 1.38–1.48 ppm (m), δ 3.28 CH_2(m) Bu_4N, δ 1.1 ppm CH_3(t) Bu_4N, δ 2.17 ppm CH_3.

2.3. Kinetics

The solvents used during the kinetic study were purified and dried prior to use by standard procedures [17]. The kinetic measurements were performed at atmospheric pressure on a GBC (Model 916) and a Varian (Cary 50) UV/Vis spectrophotometer equipped with a thermostatted 6 cell changer (0.1 °C). The oxidative addition reactions with CH_3I were followed at 425.0 nm with the exception of acetonitrile and dichloromethane, which were followed at 420.0 nm. Typical experimental conditions were [Ir_2-complex] = $0.5\text{–}5.5\times10^{-4}$ M and [CH_3I] varied between 1.0×10^{-2} and 0.2 M thus ensuring good pseudo-first-order plots of $\ln(A_t - A_\infty)$ versus time where A_t and A_∞ are the absorbencies at time t and infinity, respectively. The observed pseudo-first-order rate constants where calculated from the above plots by using a non-linear least-square program. The spectrophotometric determination of the equilibrium constant were performed similarly to previous work [14] at $\lambda = 425$ nm in acetone. The metal complex solutions were freshly prepared before each experiment to minimise the extent of the solvolysis reaction.

3. Results and discussion

3.1. Synthesis

The slight variation in the synthesis of the [Ir(μ-Cl)-(η⁴-cod)]$_2$ complex, namely the initial reduction of $H_2[IrCl_6]\cdot xH_2O$ with hydroquinone, followed by the addition of cod resulted in the formation of a pure orange crystalline product whereas the method of Bezman and Baird always yielded a mixture of orange and brown crystals. The slight variation in the synthesis of the $Bu_4N[Ir_2(\mu\text{-Dcbp})(cod)_2]$ complex also gave better yields. The neutralisation of the pyrazole-3,5-dicarboxylic acid with Bu_4NOH had the dual benefit of neutralising the acid and acting as cation for the final product. The $\nu_{(OCO)}$ of 1642 cm^{-1} compares favourably with that obtained by Bayón et al. but is a little higher than the value obtained for the corresponding rhodium(I) complex ($\nu_{(OCO)} = 1631$ cm^{-1}) indicating higher electron density in the Rh–O bond compared to that in the Ir–O bond.

A small chemical shift for all the protons in the oxidative addition product indicates a change in the chemical environment within the product compared to that of the starting material. The methyl oxidative protons at δ 2.17 ppm corresponds well with the values 2.17 and 2.20 for the mono nuclear oxidative addition products of [Ir(LL)(cod)] complexes LL = 2-pyridinethiolato-N-oxide (hpt) and

N-methyl-4-methoxybenzothiohydroxamate (AnMetha), respectively [18].

3.2. Kinetics

The proposed reaction mechanism for the oxidative addition of CH_3I to $Bu_4N[Ir_2(\mu\text{-Dcbp})(cod)_2]$ (Scheme 1) involves two different pathways namely the k_1/k_{-1} pathway (direct route) and the k_2/k_3 or solvent-assisted pathway. The k_1 and k_{-1} reaction steps can occur on their own or together with the solvent-assisted pathway.

Although only one relative slow reaction was detected for the oxidative addition of CH_3I to $Bu_4N[Ir_2(\mu\text{-Dcbp})(cod)_2]$, the possibility of a fast reaction exists because in the case of dimeric complexes both metal ions can undergo oxidative addition. The presence of a fast reaction was investigated with a stopped-flow method, but the results were inconclusive. We therefore decided upon a two-center addition of the iodomethane to give an Ir(II)–Ir(II) complex with the possibility of a metal–metal bond to fulfil 18 electron stability. Similar asymmetric alkyl halide addition have been observed for $[(PPh_3)(CO)Ir(Me)\text{-}(\mu\text{-}pz)_2\text{-}Ir(I)(PPh_3)(CO)]$ [6] and $[(\eta^4\text{-cod})Ir(Me)\text{-}(\mu\text{-}pz)_2\text{-}Ir(I)(\eta^4\text{-cod})]$ [7].

The isosbestic point, which was detected during the oxidative addition reaction, implies that only one product is formed during the reaction. The results for the oxidative addition reaction between $Bu_4N[Ir_2(\mu\text{-Dcbp})(cod)_2]$ and CH_3I is given in Table 2. The single reaction includes the possibility of oxidative addition on only one metal ion or simultaneous addition on both metal ions. We were unable to characterise the reaction product by means of X-ray crystallography so that the exact nature of oxidative addition (on both or on only one metal ion) is still unknown. A solvent-assisted pathway was included in the proposed mechanism because of the instability of the $Bu_4N[Ir_2(\mu\text{-Dcbp})(cod)_2]$-complex in solutions of acetonitrile, acetone, 1,2-dichloroethane, dichloromethane and chloroform.

The following rate law for the proposed mechanism in Scheme 1 was deduced with the application of the steady state approximation to the solvolysis intermediate, $[Ir_2(\mu\text{-Dcbp})(cod)_2S]^-$ [19]:

$$R = k_1[\mathrm{Ir}][CH_3I] - k_{-1}[P] + k_2[\ \mathrm{Ir}] - k_{-2}\left[\frac{k_2[\mathrm{Ir}] + k_{-3}[P]}{k_{-2} + k_3[CH_3I]}\right] \quad (1)$$

where $[Ir] = (Bu_4N)[Ir_2(\mu\text{-Dcbp})(cod)_2]$ and $[P] = (Bu_4N)\text{-}[Ir_2(\mu\text{-Dcbp})(cod)_2(CH_3)(I)]$.

Integrating Eq. (1) under the experimental conditions chosen, the observed pseudo-first-order rate constant for Eq. (1) is given by the following equation:

$$k_{obs} = k_1[CH_3I] + k_{-1} + k_2 - k_{-2}\left[\frac{k_2 + k_{-3}}{k_{-2} + k_3[CH_3I]}\right] \quad (2)$$

The k_{-3} pathway can be considered negligible small on the grounds that oxidative addition via the solvent-assisted pathway goes to completion so that Eq. (2) simplifies to Eq. (3).

$$k_{obs} = k_1[CH_3I] + k_{-1} + \frac{k_2k_3[CH_3I]}{k_{-2} + k_3[CH_3I]} \quad (3)$$

Eq. (3) consists of the two different pathways namely the k_1 and k_{-1} pathway and the k_2/k_3 pathway. The direct pathway (k_1/k_{-1}) can occur on its own or in conjunction with the solvent-assisted pathway (k_2/k_3).

When the contribution of the solvent-assisted pathway to the total rate is negligible, it means that oxidative addition mainly occurs along the direct pathway. If oxidative addition occurs via the k_1 and k_{-1} pathways in the presence of an excess CH_3I ($[CH_3I] \gg [\mathrm{Complex}]$) the rate constant for the direct pathway will be as follows:

$$k_{obs} = k_1[CH_3I] + k_{-1} \quad (4)$$

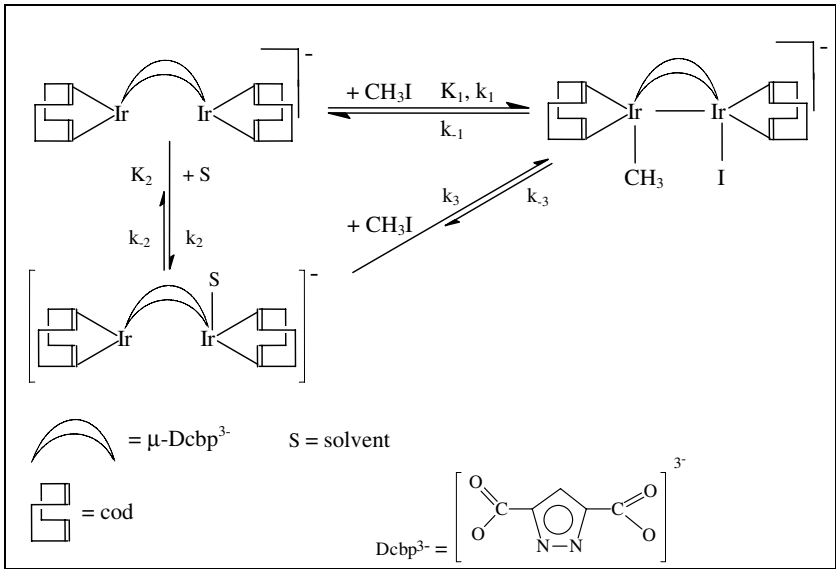

Scheme 1.

A graph of k_{obs} versus [CH_3I] will be linear with a slope equal to k_1 and an intercept equal to k_{-1}.

The results of our study however have shown that the solvent-assisted pathway contributes to the rate of oxidative addition. An example of the solvolysis reaction between $Bu_4N[Ir_2(\mu\text{-Dcbp})(cod)_2]$ and the different solvents used in this study is shown in Fig. 1 and the k_{obs} values for these reactions are listed in Table 1. A comparison between the k_{obs} value ($1.3(3)\times10^{-3}$ s^{-1} at [CH_3I] = 0) for the oxidative addition of CH_3I to $Bu_4N[Ir_2(\mu\text{-Dcbp})(cod)_2]$ in acetone and the k_{obs} value ($4.56(5)\times10^{-4}$ s^{-1}) for the reaction between acetone and $Bu_4N[Ir_2(\mu\text{-Dcbp})(cod)_2]$ show that the solvolysis reaction do not influence the rate of oxidative addition unduly. The solvolysis reactions between $Bu_4N[Ir_2(\mu\text{-Dcbp})(cod)_2]$ and 1,2-dichloroethane, chloroform and dichloromethane furthermore show isosbestic points (Table 1) which is indicative of the formation of only one product. This implies that $k_{-2} \ll k_2$ so that $k_{solv} \cong k_2$. The solvolysis complex can further react with CH_3I to form the same product which is obtained through oxidative addition by the k_1/k_{-1} pathway. A further important observation is the fact that the oxidative addition of CH_3I to $Bu_4N[Ir_2(\mu\text{-Dcbp})(cod)_2]$ shows an isosbestic point at 358.0 nm (Fig. 2) while the solvolysis reaction in Fig. 1 would probably show an isosbestic point at ~340.0 nm.

The contribution of the solvent-assisted pathway to the rate of oxidative addition was postulated as follows:

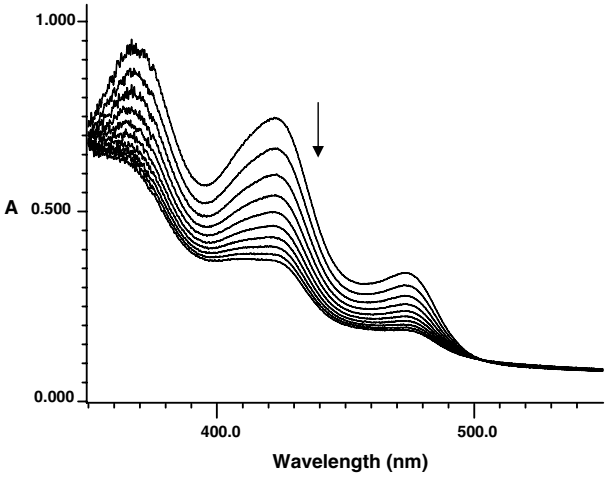

Fig. 1. Spectral changes of the $Bu_4N[Ir_2(\mu\text{-Dcbp})(cod)_2]$ complex (4.9×10^{-4} M) in acetone (10 min intervals, 25.0 °C).

Table 1
The solvolysis rate constants for $Bu_4N[Ir_2(\mu\text{-Dcbp})(cod)_2]$ in different solvents at 25.0 °C

Solvent	(10^3) k_{obs} (s^{-1})	$t_{1/2}$ (s)	Isosbestic point (nm)
1,2-Dichloroethane	0.87(3)	797	357.0
Chloroform	0.84(1)	825	359.0
Dichloromethane	0.64(3)	1083	352.0
Acetonitrile	0.51(2)	1359	
Acetone	0.456(5)	1520	

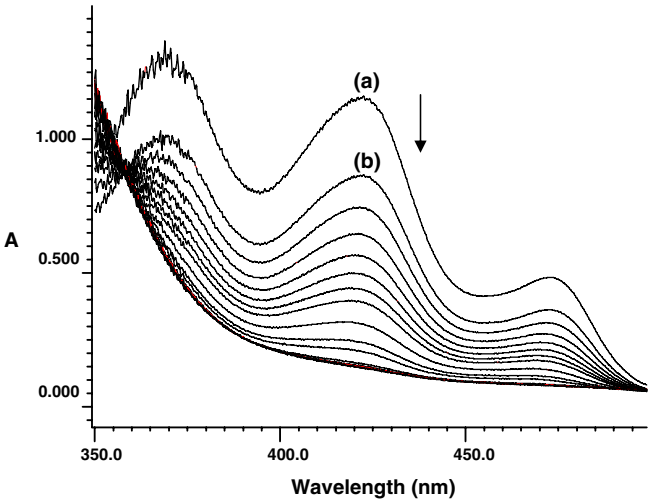

Fig. 2. (a) $(Bu_4N)[Ir_2(\mu\text{-Dcbp})(cod)_2]$ without added CH_3I in acetone; (b) spectral change for the oxidative addition of CH_3I to $(Bu_4N)[Ir_2(\mu\text{-Dcbp})(cod)_2]$ with 1 min intervals at 25 °C.

(a) If $k_3[CH_3I] \gg k_{-2}$ in Eq. (2), then Eq. (3) changes to

$$k_{obs} = k_1[CH_3I] + k_{-1} + k_2 \quad (5)$$

The intercept of Eq. (5) now contains an additional contribution, namely k_2. Eq. (5) thus implies that as soon as the solvolysis intermediate is formed, it reacts quite rapidly with CH_3I to form the expected oxidative addition product.

(b) If $k_3[CH_3I] \ll k_{-2}$ in Eq. (3), then Eq. (3) changes to

$$k_{obs} = (k_1 + k_3K_2)[CH_3I] + k_{-1} \quad (6)$$

The slope of Eq. (6) now contains contributions from the direct as well as the solvent-assisted pathway so that a graph of k_{obs} versus [CH_3I] will have a slope of $k_1 + k_3K_2$ and an intercept equal to k_{-1}. Eq. (6) implies therefore that the reaction between the solvolysis intermediate and CH_3I is quite slow.

Plots of the pseudo-first-order rate constants, k_{obs}, according to Eqs. (5) and (6) for the oxidative addition reactions against [CH_3I] in the different solvents gave linear relationships with non-zero intercepts (Fig. 3) implying reversible oxidative addition.

Eqs. (5) and (6) contain either an additional contribution towards the slope or the intercept. Both Eqs. (5) and (6) predict the same experimental results (a linear graph with a non-zero intercepts). From this it is clear that the mechanism, whether direct or a combination of direct and solvent-assisted, could not be determined from the kinetic results alone. Two further indicators, namely the difference between the oxidative addition and solvolysis rates and the isosbestic point which was observed for the oxidative addition reaction, were used to propose the mechanism in Scheme 1.

Another possibility for the direct interaction between the dinuclear iridium complex and methyl iodide is the normal S_N2 mechanism. The reaction between the metal

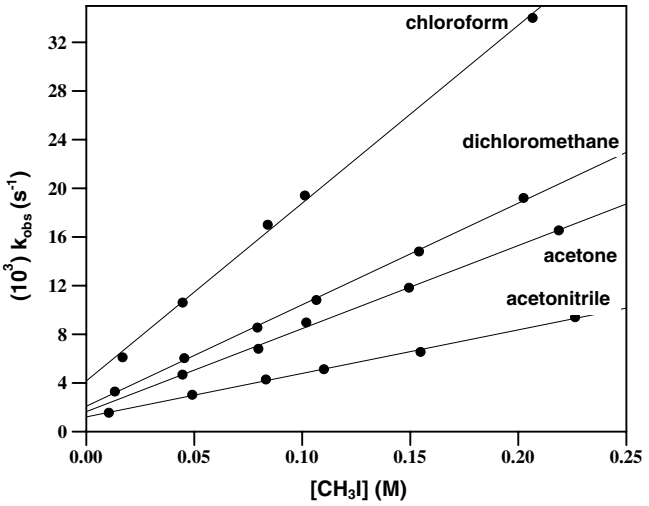

Fig. 3. k_{obs} vs. $[CH_3I]$ for the oxidative addition reaction of CH_3I with $(Bu_4N)[Ir_2(\mu\text{-Dcbp})(cod)_2]$ in different solvents (25.0 °C).

complex and the addendum molecule with the subsequent product formation is given in the following equation:

$$[Ir_2(\mu\text{-Dcbp})(cod)_2]^- + CH_3I \underset{k_{-1}}{\overset{k_1}{\rightleftarrows}} [(cod)Ir^{III}Me(\mu\text{-Dcbp})Ir^{I}(cod)],$$

$$I^- \xrightarrow{k_4} [(cod)(I)Ir^{III}\ Me(\mu\text{-Dcbp})Ir^{I}(cod)]^- \quad (7)$$

The formation of the intermediate, in close association with iodide, is most probably much faster compared to the second irreversible step $(k_1[CH_3I] + k_{-1}) \gg k_4$ [20] which results in the following rate law:

$$\text{Rate} = k_4K_1[Ir_2(\mu\text{-Dcbp})(cod)_2^-][CH_3I] \quad (8)$$

The observed rate constant for the direct interaction between the metal complex and the addendum reduces to Eq. (9) under pseudo-first-order conditions

$$k_{obs} = k_4K_1[CH_3I] \quad (9)$$

which results in a straight line for a plot of k_{obs} versus $[CH_3I]$ (see Fig. 3). The intercept which is obtained for all the different solvents are still attributed to a solvent pathway and which may include the k_2 term (see Eq. (5)). If this is true, the solvolysis rate constants and intercepts (Table 2) should be comparable within experimental error. This is not the case with the latter being constantly larger which may be interpreted that the intercepts are more complex in accordance with Eq. (5). However, the opposing solvent polarity effects (Table 2) may also be indicative of the existence of a neutral Ir(I)–Ir(III) intermediate species (vide supra) in the S_N2 process since the increase of solvent polarities lead to an unexpected 4-fold decrease in oxidative addition rates. If the Ir(I)–Ir(III) complex is maintained at steady state concentrations (as indicated by Eq. (8)) then the linear kinetic behaviour in Fig. 3 could be reconciled with the above-mentioned species' existence.

The isosbestic point which was observed for the oxidative addition of CH_3I to $(Bu_4N)[Ir_2(\mu\text{-Dcbp})(cod)_2]$ in acetone under pseudo-first-order conditions indicates the presence of only one reaction. If there is a solvolysis reaction present the contribution of this second slow reaction to the spectral changes observed in Fig. 2 is negligible small so that the spectral change is only that of oxidative addition. This explains the clearly defined isosbestic point in Fig. 2. Some uncertainty exists however because the isosbestic point for the solvolysis reaction in chloroform (356.0 nm) and that for the oxidative addition reaction (359.0 nm) in the same solvent are very close to one another. The isosbestic point for the solvolysis reaction in acetone when extrapolated occurs at a measurably lower wavelength (~340.0 nm). This reinforces the assumption that the spectral changes in Fig. 2 are only due to the oxidative addition reaction.

If Eq. (5) instead of Eq. (6) should hold, then the real value of k_{-1} can be determined by $k_{-1} = \text{intercept} - k_2$. For example a graph of k_{obs} versus $[CH_3I]$ in acetone has a slope of $7.0(1) \times 10^{-2}\ M^{-1}\ s^{-1}$ and an intercept equal to $1.3(2) \times 10^{-3}\ s^{-1}$ (Table 2). A value of $8(2) \times 10^{-4}\ s^{-1}$ is obtained for k_{-1} when k_2 is substituted with the solvolysis rate for acetone $(4.56(5) \times 10^{-4}\ s^{-1})$. According to this K_1 which is equal to $\frac{k_1}{k_{-1}}$ has a value of 88(22) M^{-1} which is similar to the spectrophotometrically determined value for K_1 of 11(2) M^{-1} if the error on both values is taken into account.

To strengthen this argument further the following experiment was performed: the complex, $(Bu_4N)[Ir_2(\mu\text{-Dcbp})(cod)_2]$ $(5.0 \times 10^{-4}\ M)$ was dissolved in acetone and left for an hour so that the solvated intermediate could form $(t_{1/2} = 25\ \text{min})$. This solution was then reacted further with

Table 2
Solvent effects for the oxidative addition of CH_3I to $Bu_4N[Ir_2(\mu\text{-Dcbp})(cod)_2]$ at 25.0 °C

Solvent	ε	$(10^2)\ k_1\ (M^{-1}\ s^{-1})$	(10^3) Intercept[a] (s^{-1})	$(10^3)\ k_2$[b] (s^{-1})	$(10^3)\ k_{-1}$[a] (s^{-1})	K[c] (M^{-1})
Chloroform	4.9	14.6(4)	4.2(4)	0.84(1)	3.4(4)	43(5)
Dichloromethane	8.9	8.3(1)	2.1(1)	0.64(3)	1.5(1)	55(4)
1,2-Dichloroethane	10.4	7.7(1)	2.4(1)	0.87(3)	1.5(1)	51(3)
Acetone	20.7	7.0(1)	1.3(2)	0.456(5)	0.8(2)	88(22) 11(2)[d]
Acetonitrile	38	3.58(7)	1.20(9)	0.51(2)	0.69(9)	52(12)

[a] $k_{-1} + k_2$.
[b] Solvolysis rate constant.
[c] $K = k_1/k_{-1}$.
[d] Spectrophotometrically.

CH_3I (0.015 M) and followed at 425.0 nm. A pseudo-first-order rate constant of $1.35 \times 10^{-3}\ s^{-1}$ ($=k_3[CH_3I]$) was obtained. This rate is a factor 3 faster than the rate obtained for k_2 ($4.56(5) \times 10^{-4}\ s^{-1}$) implying that the assumption of $k_3[CH_3I] \gg k_{-2}$ made in the deduction of Eq. (4) was justified. The fact that $k_3[CH_3I] \geqslant k_2$ further strengthens the argument for the existence of the k_3 pathway.

This solvent-assisted oxidative addition reaction is furthermore a factor 10 slower than the comparable rate for the direct pathway under the same conditions. Similar results were also obtained when this experiment was repeated with chloroform as solvent. In this case oxidative addition via the solvent-assisted pathway was a factor 40 slower than that for the direct pathway. Oxidative addition therefore occurs mainly via the direct pathway especially since the solvolysis rate constants for acetone and chloroform ($k_2 = 4.56(5) \times 10^{-4}$ and $8.4(1) \times 10^{-4}\ s^{-1}$, respectively) are relatively slow.

The intercept, which was obtained from the plots of the pseudo-first-order rate constants, k_{obs}, versus $[CH_3I]$ in the different solvents (Fig. 3), is therefore a combination of the solvolysis reaction (k_2 pathway) and reductive elimination (k_{-1} pathway). The results in Table 2 of the solvent effects show that the rate of oxidative addition depends to a slight degree on the characteristics of the different solvents. The most important being a decrease in rate constants with a simultaneous increase in dielectric constant. The observed solvent effect could however not be attributed to the donosity of the solvents.

This is in contrast to the expected solvent effect for oxidative addition reactions. Normally oxidative additions are characterised by a 20–60-fold increase in the oxidative addition rate when the solvents are varied [21]. An example of such an increase in the oxidative addition rate is the 20-fold increase in the rate constants for the oxidative addition of CH_3I to [Rh(acac)(CO)(PPh_3)] in different solvents [22]. A comparison of the solvent effect for the k_1 pathway in this case, with that observed for the oxidative addition of CH_3I to the corresponding $[Ir_2(\mu\text{-pz})_2(cod)_2]$ complex shows that the solvent effect in our case is remarkably smaller than the reported effect [23]. The increase in the oxidative addition rate in this study is 4-fold while in the case of $[Ir_2(\mu\text{-pz})_2(cod)_2]$ there is a 16-fold increase in the rate constants. Our results also compare with an increase of approximately a factor 9 which was observed for the oxidative addition reaction between the monomeric [Ir(hpt)(cod)] complex and iodomethane and an increase of a factor 4 for the corresponding reaction between [Ir(AnMetha)(cod)] and iodomethane [18].

The solvent effect for the oxidative addition reactions observed here is also strongly reminiscent to that of [Ir(hpt)(cod)] and [Ir(AnMetha)(cod)] [18] where negative intrinsic volumes of activation, supported by a significant reduced angle (156°) for the *trans*-orientated H_3C–Ir(III)-I moiety in the oxidative addition products [24,25], pointed to a linear S_N2 transition state of $[Ir\cdots CH_3\text{–}I]^{\neq}$ for the k_1 pathway. This non-linear orientation was due to steric crowding of the cod ligand's methylene protons above and below the plane formed by the iridium and the ancillary bidentate ligand atoms. We envisaged the same phenomenon in the present complex in that the rate of initial nucleophilic attack of the metal upon the methyl carbon in CH_3I is slowed down due to the above-mentioned steric crowding. This may also be the reason why the solvolysis reaction becomes more pronounced relative to the oxidative addition rate.

The activation parameters, $\Delta H^{\neq}$ and $\Delta S^{\neq}$, for the oxidative addition of CH_3I to $(Bu_4N)[Ir_2(\mu\text{-Dcbp})(cod)_2]$ (k_1 pathway) are $47(2)\ kJ\ mol^{-1}$ and $-110(7)\ JK^{-1}\ mol^{-1}$, respectively. The activation parameters for the reductive elimination reaction (k_{-1} pathway) were not determined because the intercept values in Table 2 are a combination of the k_{-1} and the k_2/k_3 pathways. The fairly negative entropy of activation together with the positive enthalpy of activation is indicative of an associative process which is more enthalpy than entropy driven for the k_1 pathway.

The enthalpy of activation for the k_1 pathway is similar to the values which was reported for the corresponding $[Ir_2(\mu\text{-pz})_2(cod)_2]$ complex [23]. There are however a big difference in the entropy of activation being zero within experimental error in the case of the $[Ir_2(\mu\text{-pz})_2(cod)_2]$ complex ($15(25)\ J\ K^{-1}\ mol^{-1}$). Both the entropy and the enthalpy values of activation for the $(Bu_4N)[Ir_2(\mu\text{-Dcbp})(cod)_2]$ complex is also in agreement with the general activation parameters which was reported for the corresponding monomeric iridium(I) complexes [26].

Acknowledgements

The authors thank the South African Foundation for Research Development as well as the Research Fund of this University for financial support.

References

[1] A.P. Sadimenko, S.S. Basson, Coord. Chem. Rev. 147 (1996) 247.
[2] M.P. García, M.A. Esteruelas, M. Martin, L.A. Oro, J. Organomet. Chem. 467 (1994) 151.
[3] M. A Esteruelas, M.P. García, A.M. López, L.A. Oro, Organometallics 10 (1991) 127.
[4] M.P. Garcia, A.M. López, M.A. Esteruelas, F.J. Lahoz, L.A. Oro, J. Chem. Soc., Chem. Commun. (1988) 793.
[5] M.A. Esteruelas, M. P Garcia, A.M. López, L.A. Oro, Organometallics 11 (1992) 702.
[6] K.A. Beveridge, G.W. Bushnell, K.R. Dixon, D.T. Eadie, S.R. Stobart, J. Am. Chem. Soc. 104 (1982) 920.
[7] A.W. Coleman, D.T. Eadie, S.R. Stobart, J. Am. Chem. Soc. 104 (1982) 922.
[8] J.L. Atwood, K.A. Beveridge, G.W. Bushnell, K.R. Dixon, D.T. Eadie, S.R. Stobart, M.J. Zaworotko, Inorg. Chem. 23 (1984) 4050.
[9] K.A. Beveridge, G.W. Bushnell, S.R. Stobart, Organometallics 2 (1983) 1447.
[10] D.O.K. Fjeldsted, S.R. Stobart, M.J. Zaworotko, J. Am. Chem. Soc. 107 (1985) 825.
[11] J.A. Bailey, S.L. Grundy, S.R. Stobart, Organometallics 9 (1990) 536.

[12] G.W. Bushnell, D.O.K. Fjeldsted, S.R. Stobart, J. Wang, Organometallics 15 (1996) 3785.
[13] T.G. Schenk, C.R.C. Milne, J.F. Sawyer, B. Bosnich, Inorg. Chem. 24 (1985) 2338.
[14] S.S. Basson, J.G. Leipoldt, W. Purcell, J.B. Schoeman, Inorg. Chim. Acta 173 (1990) 155.
[15] S.A. Bezman, P.H. Bird, A.R. Fraser, J.A. Osborn, Inorg. Chem. 19 (1980) 3755.
[16] J.C. Bayón, G. Net, P. Esteban, P.G. Rasmussen, D.F. Bergstorm, Inorg. Chem. 30 (1991) 4771.
[17] D.D. Perrin, W.L.F. Armarego, Purification of Laboratory Chemicals, 3rd ed., Pergamon Press, Oxford, 1988.
[18] M. Theron, E. Grobbelaar, W. Purcell, S.S. Basson, Inorg. Chim. Acta 358 (2005) 2457.
[19] A. Wojcicki, Adv. Organomet. Chem. 11 (1973) 87.
[20] J.H. Espenson, Chemical Kinetics and Reaction Mechanisms, 2nd ed., McGraw-Hill, New York, 1995, pp. 86–90.
[21] S.S. Basson, J.G. Leipoldt, J.T. Nel, Inorg. Chim. Acta 167 (1984) 84.
[22] J.G. Leipoldt, S.S. Basson, L.J. Botha, Inorg. Chim. Acta 215 (1990) 168.
[23] R.D. Brost, S.R. Stobart, J. Chem. Soc., Chem. Commun. (1989) 498.
[24] S.S. Basson, J.G. Leipoldt, W. Purcell, J.B. Schoeman, Acta Crystallogr., Sect. C 45 (1989) 2000.
[25] Y.M. Terblans, S.S. Basson, W. Purcell, G.J. Lamprecht, Acta Crystallogr., Sect. C 51 (1995) 1748.
[26] K.G. van Aswegen, J.G. Leipoldt, I.M. Potgieter, G.J. Lamprecht, A. Roodt, G.J. van Zyl, Transit. Met. Chem. 16 (1991) 369.